Chapter II

Literature review

There are numerous number of literature available for removal of SO_2 and NO individually. Several processes have been used for simultaneous removal of SO_2 and NO from contaminated gas stream. Some recent literatures for simultaneous removal of SO_2 and NO for simulated flue gas in wet process are discussed in this section.

2.1. Removal by using a complex mixture of Ha-Na/$NaClO_2$

Hao et al., 2017 proposed an integrated and efficient wet technology to remove SO_2 and NO simultaneously. Here a complex absorbent consisting of sodium humate (Ha-Na) and sodium chlorite ($NaClO_2$) with effective mass concentration ratio of 4:0.7 in terms of percentage was used. The experiments were performed at ambient pressure in a bubbling reactor (I.D. 70 mm; height 150 mm), where the reaction temperature was controlled with use of water bath. The reaction temperature, absorbent pH, the coexistence of gases, absorbent mass concentration and the soluble anions were significant factors, examined during the experimentation. The characteristic reaction mechanism was also explained. The schematic view of experimental setup was shown below in Figure 2.1. It has shown

effective removal efficiency of 98-99 and 98 % for SO_2 and NO, respectively, for maintained initial concentration below 35 mg/m^3 with the complex absorbent. Here the S(IV) species promoted NO_2 absorption where Cl^-, HCO_3^-, CO_3^{2-} and NO_2^- constrained the NO conversion. The products after absorption of SO_2 and NO were recognized as humic, nitrate and sulfate by X-ray diffraction (XRD), X-ray photoelectron spectroscopy (XPS) and Fourier transform Infrared radiation (FT-IR) characterizations.

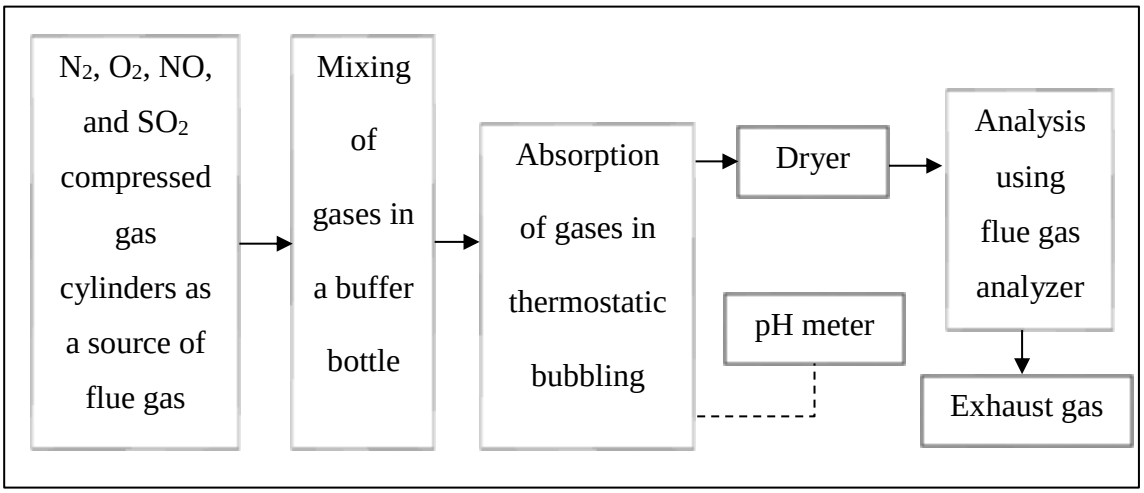

Figure 2.1. Schematic for absorption of SO_2 and NO in a bubbling reactor using Ha-Na/$NaClO_2$

2.2. Absorption using ammonia-Fe(II)EDTA for sintering plants

The combined removal of SO_2 and NO from sintering flue gases using ammonia-Fe(II) EDTA was studied by Wang et al., 2017. The process was carried out in a pilot scale absorption chamber with simulated sintering flue gas stream at different operating parameters. The major operating parameters used for the process were sintering flue gas

flow rate, flue gas temperature, slurry oxidation, SO_2 and NO concentrations. The process consisting of absorption, control, flue gas preparation, heating, regeneration, slurry compounding and test unit was shown in Figure 2.2. The analyses of SO_2 and NO concentrations were done by using an online infrared flue gas analyser. The pH of the absorbent in absorption chamber was adjusted with oxidation-reduction potential (ORP) pH meter. The maximum removal efficiencies obtained in the experimentation were 94.41 and 54.77 % for SO_2 and NO, respectively. The process conveys that increase in flue gas flow rate, oxidation air flow rate and NO concentration has negative effect in NO removal efficiency. The reaction temperature has negligible effect on the combined removal of SO_2 and NO. Combined absorption of SO_2 and NO has minute change with increase in initial SO_2 concentration in the flue gas stream.

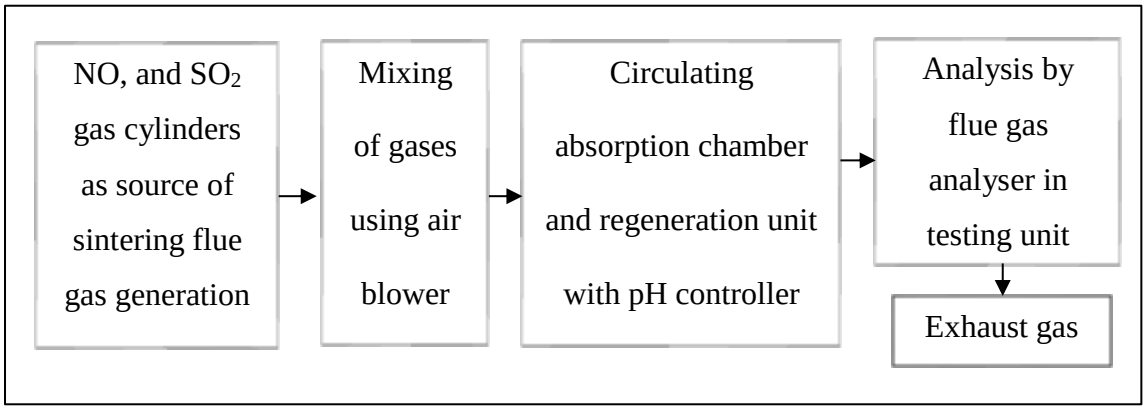

Figure 2.2. The process for SO_2 and NO absorption using ammonia-Fe(II)EDTA for sintering plants

2.3. Rotating drum biofilter coupled with complexing absorption by Fe^{II}(EDTA)

In the study of Chen et al., 2016, an emerging process for combined removal of SO_2 and NO was examined in a rotating drum bio filter with complex absorbent integrated with microbial process. The process is concerned about use of Fe^{II}(EDTA) as solvent to increase the mass transfer of NO and also to employ denitrifying bacteria and sulphate reducing bacteria for denitrification and desulfurization, respectively. The various operating parametric tests performed during the process were addition of microbial community, empty bed residence time, inlet SO_2 concentration, NO concentration, and O_2 concentration to investigate their influence on performance of the bioreactor. The process outline was shown in Figure 2.3. The rotating drum bio filter process was incorporated with gas supply unit, inspection section unit and the absorption unit. The process was initiated with enriched culture media for reduction of sulphate and nitrate by the bacteria in the biofilm.

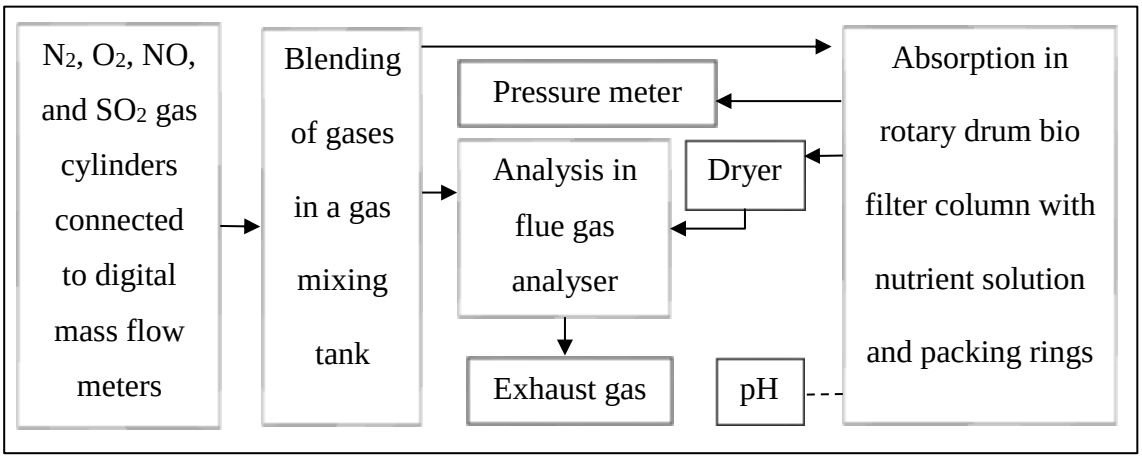

Figure 2.3. Absorption of SO_2 and NO in rotating drum biofilter using Fe^{II}(EDTA) as absorbent

The 10 mM Fe^{II}(EDTA) has great impact on NO removal efficiency in the 60-day process. During the parametric tests, the maximal removal efficiency was attained 98.5 and 93% for SO_2 and NO, respectively. The results were obtained at process conditions of 1.8 min empty bed residence time, 800 mg/m^3 NO, 2 vol. % oxygen and 2000 mg/m^3 SO_2 concentration. The process conveyed that *Pseudomonas* was dominant microbial for NO removal where as *Desulfovibrio* was microbial for SO_2 removal with maximum abundance in nutrient solution.

2.4. Absorption in pilot-scale reactor using NH_3-Fe(II)EDTA

Zhang et al., 2016 reported combined SO_2 and NO absorption using ammonia-Fe(II)EDTA absorption to get valuable data for scaling up the process useful to industrialization. In this process, the applied operating conditions of the sintering plant were replicated in a small-scale pilot-scale reactor to evaluate the effect of absorbent properties on SO_2 and NO combined removal. The process flow sheet was given in Figure 2.4. The Fe(II)EDTA concentration, $(NH_4)_2SO_4$ concentration, $(NH_4)_2SO_3$ concentration, SO_3^{2-} concentration, Cl^- concentration and absorbent temperature were the major operation variables during the process of combined removal of SO_2 and NO. The absorption of NO was complicated in presence of $(NH_4)_2SO_4$ concentration and high absorbent temperature. The maximum removal efficiency of 100 and 90.63% was obtained for SO_2 and NO, respectively during the process. There is a removal efficiency drop of NO with increase in $(NH_4)_2SO_4$ concentration. Fe(II)EDTA concentration, SO_3^{2-} concentration and pH has positive impact towards NO removal. Particularly the presence of SO_3^{2-} ions in absorbent solution effectively increased the life of chelating agents. The chloride ions stick to neutral effect during combined absorption of SO_2 and NO.

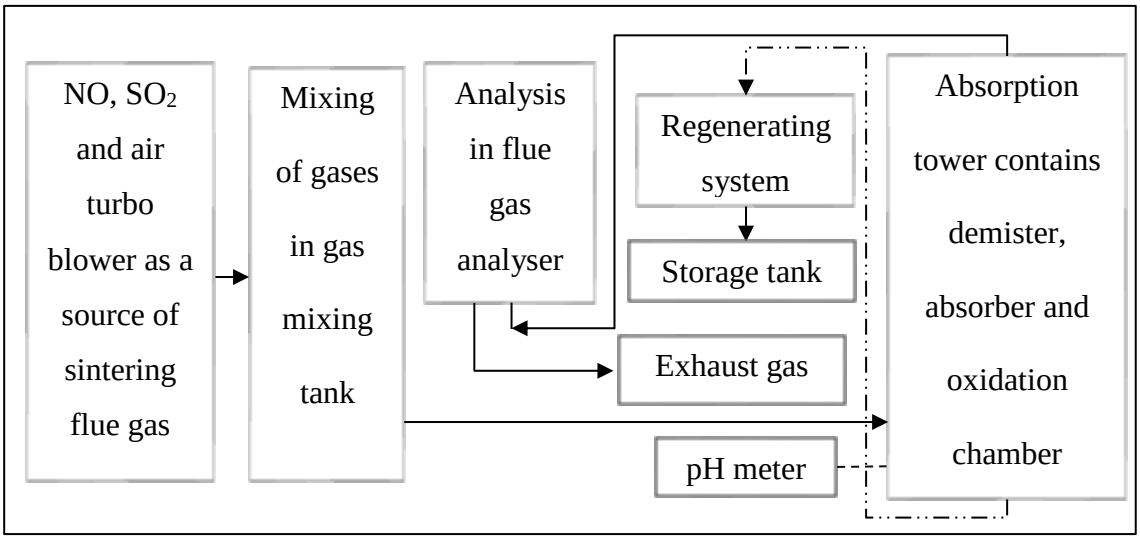

Figure 2.4. Experimental flow sheet for absorption of SO_2 and NO using ammonia-Fe(II)EDTA

2.5. Integrative pre-oxidation and post-absorption with a cost-effective complex oxidant

In the work of Zhao et al. 2016, a unique process combining pre-oxidation and post-absorption was adapted for multi component removal in flue gas stream containing SO_2, NO and Hg^0. Here a complex cost-effective oxidant containing mixer of H_2O_2 and $NaClO_2$ was used to oxidize Hg^0 and NO followed by absorption of oxidation products in $Ca(OH)_2$ slurry. The optimal conditions for the reaction were established by varying the operating parameters such as adding rate of complex oxidant, concentrations of coexistence gases, flue gas residence time, molar ratio of H_2O_2 to $NaClO_2$ in complex oxidant, pH of complex oxidant and the reaction temperature for simultaneous removal of SO_2, NO and Hg°. The schematic process flow sheet was shown in Figure 2.5. The experiments were performed in a fixed-bed reactor consisting of the simulated flue gas

generation, complex oxidant vaporization with air pollutants oxidation, absorption and tail gas detection. The experimental results had showed constant desulfurization in all parametric tests but the NO and Hg^0 removal was initially affected by addition of $NaClO_2$ followed by the complex oxidant concentration, pH, and the operating temperature. Here NO and SO_2 were also characterized as the Hg^0 removal promoters. The maximum removal efficiencies were observed for SO_2, NO and Hg^0 as 100, 87 and 92%, respectively at optimal reaction conditions. The removal products were characterized by Atomic Fluorescence Spectroscopy (AFS), Energy-dispersive X-ray spectroscopy (EDX), Ultraviolet–visible spectroscopy (UV–vis), XPS and XRD.

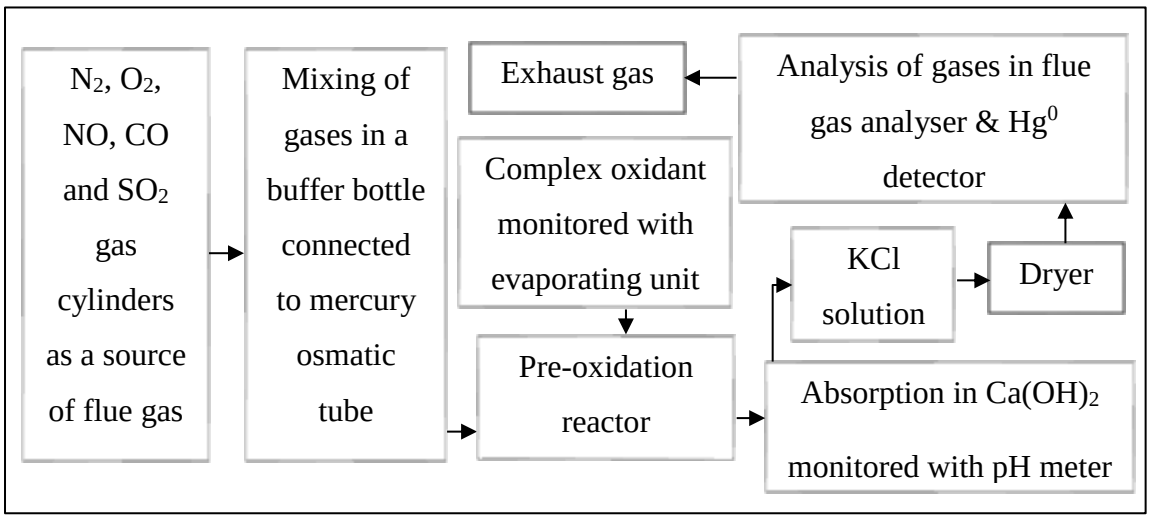

Figure 2.5. Experimental flow sheet for SO_2, NO and Hg^0 removal by integrative pre-oxidation and post-absorption

2.6. Removal by combined persulfate and ferrous–EDTA solutions

Adewuyi and Khan 2016 studied the effects of persulfate and EDTA concentrations with varying temperature and pH on the removal of NO merged with SO_2 gas stream using $Na_2S_2O_8/Fe^{2+}$-EDTA aqueous solutions. The process diagram adopted in this work was shown in Figure 2.6. The absorption was done in a jacketed Pyrex glass bubble column (I.D. 5.1 cm; length 61cm). The increase of temperature and $Na_2S_2O_8$ concentration has positive effect in removal efficiency but EDTA has antagonistic effects with rise in temperature. The obtained optimal conditions for the process were 313-323 K reaction temperature, 0.01M Fe^{2+}, 0.10 M $Na_2S_2O_8$, 60.01 M EDTA and pH range of 6-8. The obtained maximum NO removal was 96.28%.

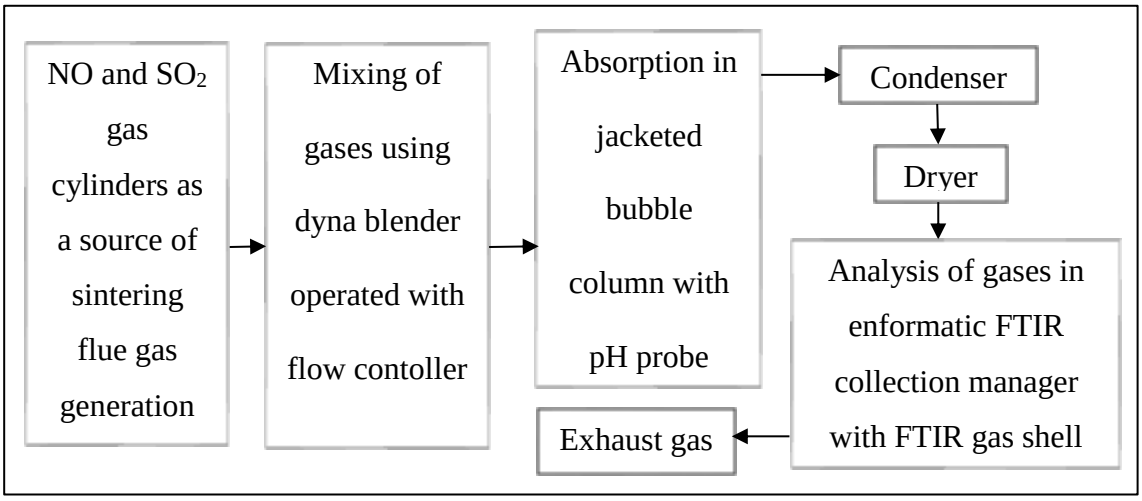

Figure 2.6. Experimental flow sheet for removal of SO_2 and NO by combined $Na_2S_2O_8/Fe^{2+}$-EDTA solutions

2.7. Wet scrubbing combined with a plasma electrostatic precipitator

A novel process was studied by Park et al., 2015 for simultaneous SO_2 and NO removal using a wet scrubber merged with an electrostatic precipitator. During the process, wet scrubber was employed for absorption of SO_2 and NO where as non-thermal plasma was used to electrostatic aerosol precipitation. SO_2 and NO gases were absorbed in wet scrubber by aerosol particles of $NaClO_2$ solution. The experimental flow sheet for the process was shown in the **Figure 2.7.**

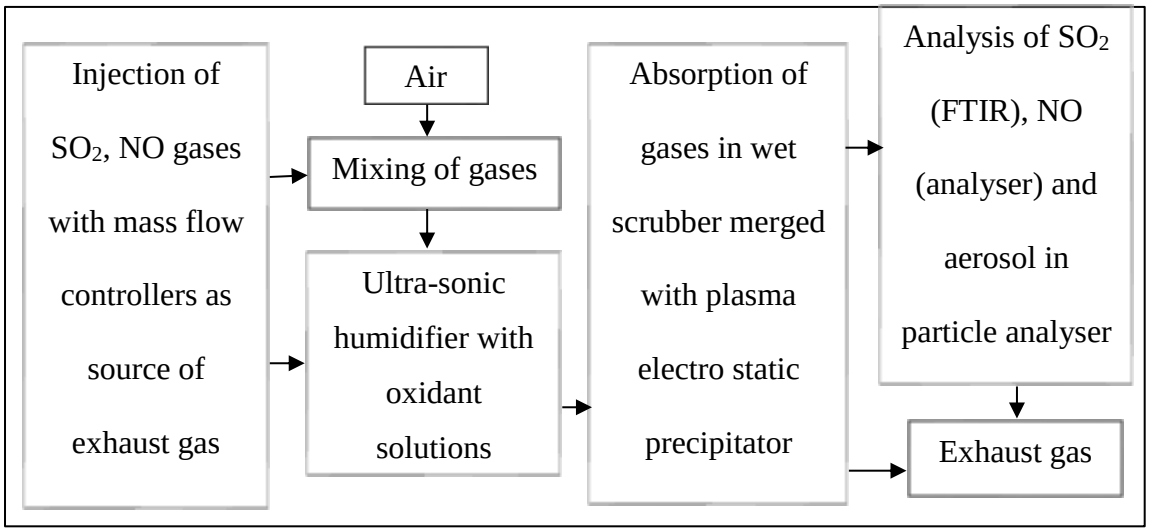

Figure 2.7. Process flow sheet for wet scrubbing of SO_2 and NO combined with a plasma electrostatic precipitator

During the absorption of SO_2 and NO with $NaClO_2$ solution, the aerosol particles were generated in form of NO_2^-, NO_3^-, HSO_3^-, and SO_4^{2-} aqueous ions. The negatively charged aerosol particles were collected on the surface of anode grounded in the plasma electrostatic precipitator. The process showed efficient absorption as 94.4% NO and

100% SO_2 removal at 500 mg/m^3 gas concentrations and a 60 Nm^3/h total gas flow rate. The operating $NaClO_2$ molar flow rate was 50 mmol/min and the gas–liquid contact time was 1.25 S. At maximum plasma power input of 68.8 W, the aerosol particles in the exit gas were minimized to 7.553 µg/m^3 and 210 µg/cm^3 which resembled the values for clean air. The major reactions occurred during the process were given below:

$$4NO + 3ClO_2^- + 2H_2O \rightarrow 4HNO_3 + 3Cl^- \quad \Delta G = -640 \text{ kJ/mol.} \qquad (2.1)$$

$$2SO_2 + ClO_2^- + 2H_2O \rightarrow 2H_2SO_4 + Cl^- \quad \Delta G = -450 \text{ kJ/mol.} \qquad (2.2)$$

2.8. Removal by ferrate (VI) solution

Zhao et al., 2014 investigated the simultaneous removal of SO_2, NO and Hg^0 from exhaust gas by ferrate (VI) solution in a bubbling reactor as shown in Figure 2.8. The influencing operating conditions studied for the process were gas flowrate, absorbent concentration and reaction temperature. The best results for removal efficiencies of SO_2, NO and Hg^0 were 100, 64.8 and 81.4%, respectively for combined removal of SO_2 and NO using ferrate solution. The optimal conditions obtained for the process were 1 L/min of flue gas flow rate, 0.25 mmol/L of ferrate (VI) solution, 8.0 of pH and reaction temperature of 320 K. Standard electrode potential (E_0) based on the characteristics of the ferrate (VI) solution with E_0 values of reactants were also proposed. FeO_4^{2-} and $HFeO_4^-$ are the dominating species in liquid absorbent to obtain SO_4^{2-}, NO_3^- and Hg^{2+} during combined SO_2, NO and Hg^0 removal. The major reactions involved in the process were as follows:

$$HFeO_4^- \leftrightarrow H^+ + FeO_4^{2-} \qquad pK_a = 7.3 \qquad (2.3)$$

$$SO_2 + 3\,FeO_4^{2-} + 5H_2O \leftrightarrow SO_4^{2-} + 3\,Fe(OH)_3 + OH^- + 5/2\,O_2 \qquad (2.4)$$

$$SO_2 + 3\,HFeO_4^{2-} + 7/2\,H_2O \leftrightarrow SO_4^{2-} + 3\,Fe(OH)_3 + OH^- + 7/4\,O_2 \qquad (2.5)$$

$$NO + 3\,FeO_4^{2-} + 4\,H_2O \leftrightarrow NO_3^- + 3\,Fe(OH)_3 + 2OH^- + 3/2\,O_2 \quad (2.6)$$

$$NO + 2\,HFeO_4^{2-} + 3\,H_2O \leftrightarrow NO_3^- + 2\,Fe(OH)_3 + 2\,OH^- + 1/2\,O_2 \quad (2.7)$$

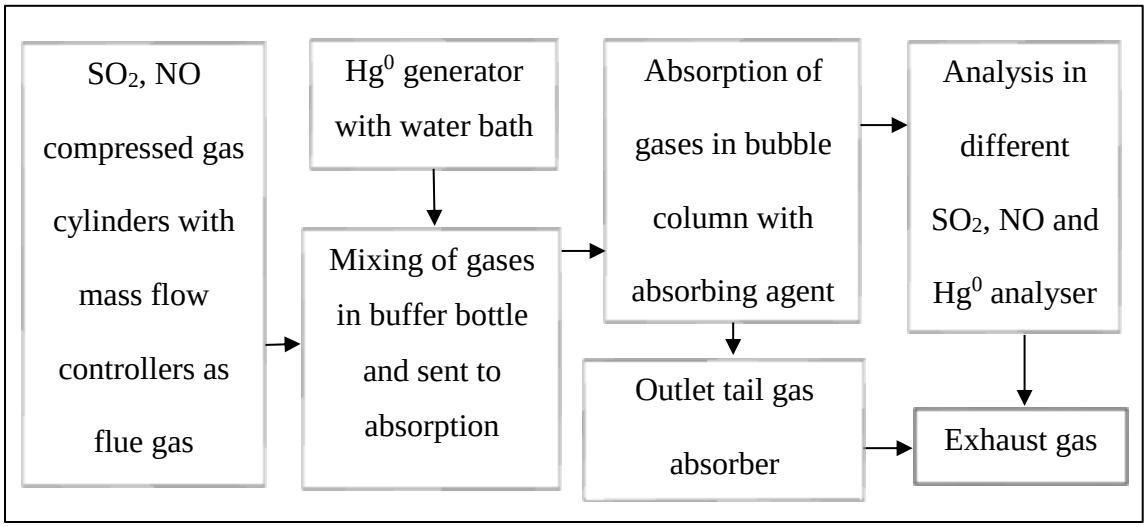

Figure 2.8. Process flow sheet for removal of SO_2 and NO by ferrate (VI) solution

2.9. Advanced oxidation using ultraviolet/H_2O_2/NaOH process

The absorption performance of SO_2 and NO by using UV/H_2O_2 advanced oxidation combining with alkalis was investigated by Liu et al., 2014. NaOH is considered as alkali in this process due to better transmittance than $Ca(OH)_2$. The effect of various influencing factors such as energy density per unit solution, gas flow, reaction temperature, Fe^{2+}, H_2O_2, NaOH, NO, O_2, SO_2, and t-butanol concentrations was studied for combined removal of SO_2 and NO. The experimentation was done in a jacketed Perspex photo-chemical bubbling reactor (hight 40 cm; I.D. 8 cm) with simulated flue gas generation and analysis system as shown in Figure 2.9. The results had shown complete SO_2 removal

in all operating conditions. Increase in energy density per unit solution, H_2O_2, NaOH, and t-butanol concentrations promoted NO removal. Increase in gas flow rate, NO and Fe^{2+}concentration reduced NO removal efficiency. Slight change was observed in NO removal by increasing SO_2, O_2 concentrations and reaction temperature. The OH^- free radicals play an effective role in NO oxidation during the process and oxidation by H_2O_2 has secondary impact on the process. The final reaction product during the experimentation was NO_3^-.

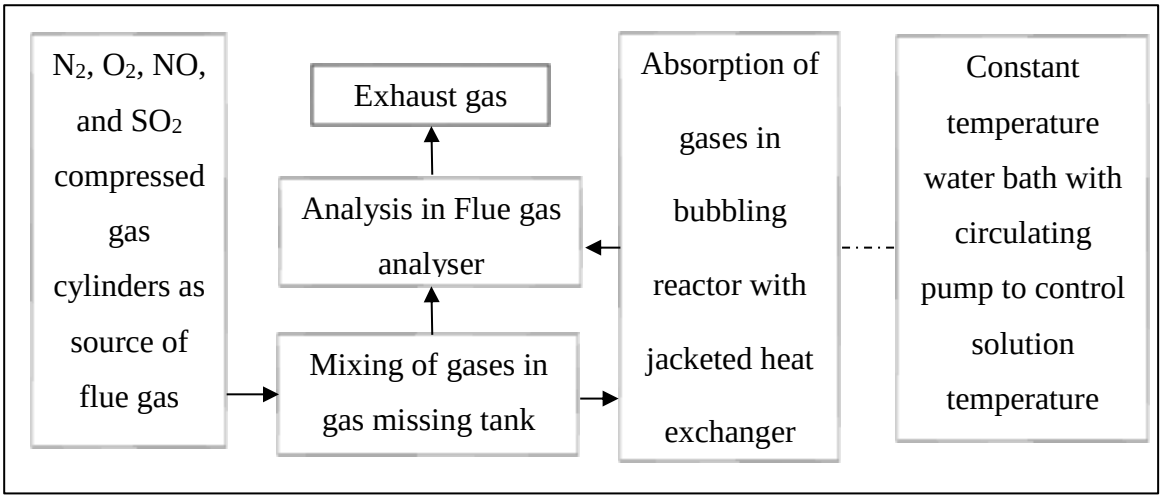

Figure 2.9. Process flow sheet for SO_2 and NO removal by advanced oxidation using ultraviolet/H_2O_2/NaOH

2.10. Removal by wet scrubbing using urea solution

Fang et al., 2011 investigated the fundamental study of theory and treatment technology for combined SO_2 and NO removal using urea solution. The experiments were conducted in a borosilicate glass packed column (I.D. 5 cm; length 1.2 m) with counter current

continuous mode operation. During the process, the SO_2 and NO_X removal efficiencies were emphatically measured under various influencing factors such as temperature, pH, oxidation degree of NO_X, SO_2, urea concentrations and additive to absorbent. Process flow diagram was detailed in Figure 2.10**.**

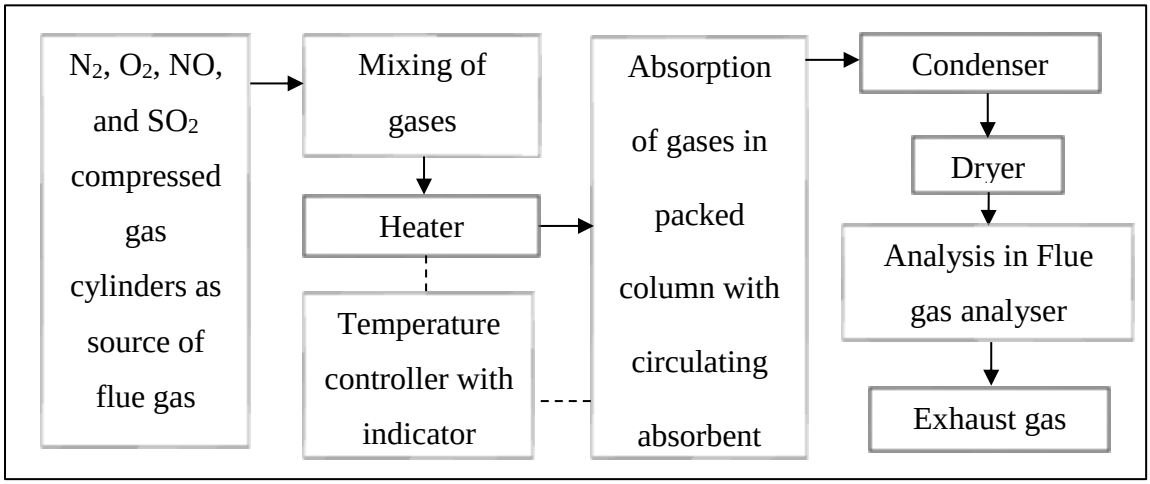

Figure 2.10. Experimental flow sheet for removal of SO_2 and NO by wet scrubbing using urea solution

The SO_2 was removed up to its maximum 100% with optimal conditions but NO was successfully removed up to 40% by urea solution. The additive increases the removal efficiency to 50%. The optimal conditions were established as 333 K reaction temperature, 5–9 solution pH, 5–10 wt.% urea concentration and 1% additive (H_2O_2 or $NaClO_2$). The reaction mechanism of the process was given for combined removal of SO_2 and NO using urea solution and reaction products. The reactions of SO_2 and NO_x with $(NH_2)_2CO$ in solution are:

$$SO_2 + (NH_2)_2CO + 2H_2O + \frac{1}{2}O_2 \rightarrow (NH_4)_2SO_4 + CO_2 \quad (2.8)$$

$$NO + NO_2 + (NH_2)_2CO \rightarrow 2N_2 + CO_2 + 2H_2O \quad (2.9)$$

2.11. Absorption in liquid phase with new complex Absorbent ($NaClO/NaClO_2$)

The effect of a new complex absorbent i.e. using a solution blend of NaClO and $NaClO_2$ for simultaneous desulphurization and denitrification in liquid phase was carried out by Zhao et al., 2011 by using self-fabricated bench scale bubbling reactor. General schematic procedure is given in Figure 2.11. The major operating parameters pH, molar ratio, temperature and concentration of the absorbent were studied for simultaneous removal of SO_2 and NO and effective removal percentages are 100 and 89.2 %, respectively. Kinetics of the process was proposed. Thermodynamic parameters i.e. enthalpy changes, Gibbs free energy and equilibrium constants for the process were calculated and showed the feasibility of the process. SO_3 and Cl_2 were generated in the oxidation of SO_2 with the help of $NaClO_2$ as oxidant. The reactions occurred during simultaneous absorption of SO_2 and NO in the process were listed as:

$$ClO_2 + SO_2 \rightarrow SO_3 + ClO \quad (2.10)$$

$$ClO + SO_2 \rightarrow SO_3 + Cl \quad (2.11)$$

$$ClO_2 + NO \rightarrow NO_2 + ClO \quad (2.12)$$

$$ClO + NO \rightarrow NO_2 + Cl \quad (2.13)$$

$$Cl + NO \rightarrow ClNO \quad (2.14)$$

$$Cl + NO_2 \rightarrow ClNO_2 \quad (2.15)$$

$$Cl + Cl \rightarrow Cl_2 \quad (2.16)$$

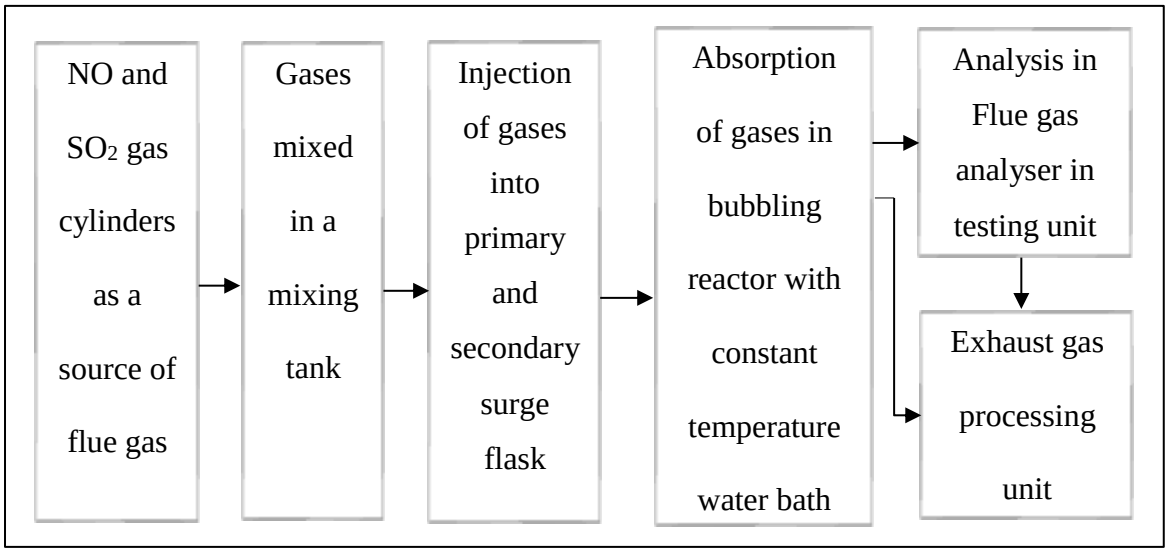

Fig. 2.11. Process flow sheet of SO_2 and NO absorption in liquid phase with new complex absorbent.

2.12. Pyrolusite slurry absorption combined with gas-phase oxidation

The work carried out by Wei-yi et al., 2011 was based on studied combined absorption of NO_x and SO_2 in pyrolusite slurry with integrated gas-phase oxidation using ozone. The study was conducted in a combined cylindrical ozonizing chamber (I.D. 5 cm; length 25 cm) and bubbling reactor (I.D. 18.5 cm; height 38 cm) as shown in Figure 2.12. The continuous stirring for the process was provided by mechanical agitator with speed of 300 rpm. The major operating parameters tested for the process were injected ozone, NO, pyrolusite concentrations, reaction temperature and rate of Mn extraction on NO_x/SO_2 removal efficiency. Here ozone successfully oxidises NO to NO_2 with high selectivity followed by MnO_2 in pyrolusite slurry could convert SO_2 to $MnSO_4$ and NO_2 to $Mn(NO_3)_2$ in liquid phase. NO_x removal efficiency was promoted with increase in ozone concentration. The process reactions were given below:

$$MnO_2 + SO_2 \rightarrow Mn^{2+} + SO_4^{2-} \quad (2.17)$$

$$SO_2 + H_2O + (½)\ O_2 \rightarrow 2H+ + SO_4^{2-} \quad (2.18)$$

$$MnO_2 + 2NO_2 \rightarrow Mn^{2+} + 2NO_3^- \quad (2.19)$$

$$(½)O_2 + 2NO_2 + H_2O \rightarrow 2H^+ + 2NO_3^- \quad (2.20)$$

$$H^+ + MnO_2 + HNO_2 \rightarrow Mn^{2+} + NO_3^- + H_2O \quad (2.21)$$

$$O_2 + 2HNO_2 \rightarrow 2H^+ + 2NO_3^- \quad (2.22)$$

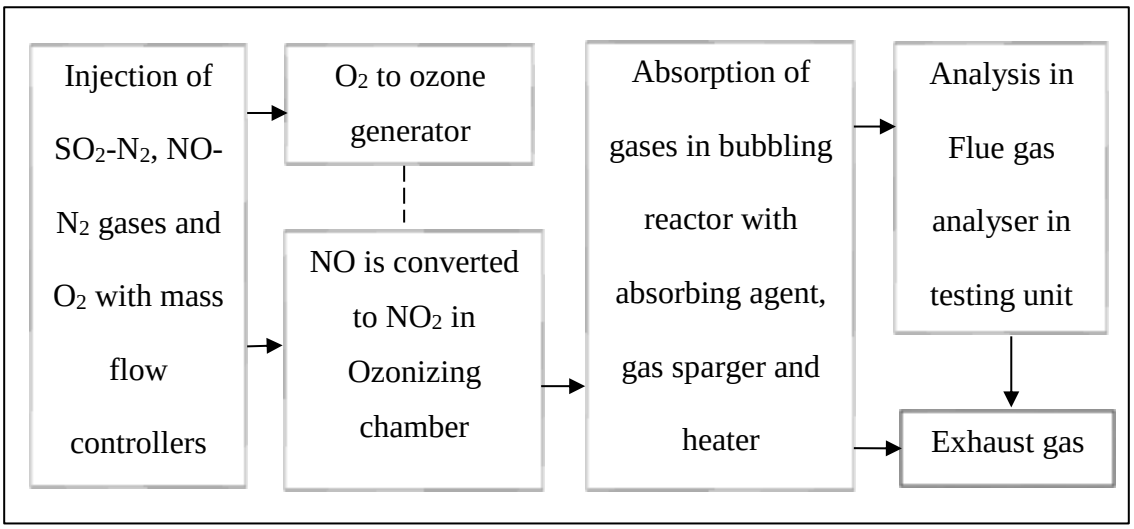

Figure 2.12. Absorption of SO_2 and NO into pyrolusite slurry combined with gas-phase oxidation ozone

2.13. Advanced oxidation using UV/H_2O_2

The study of Liu et al., 2010 was focused on the absorption performance of SO_2 and NO by using UV/H_2O_2 advanced oxidation. Various influencing factors investigated for combined removal of SO_2 and NO were variation of UV lamp power, H_2O_2 concentration and time. The experimentation was done in a Poly methyl methacrylate (PMMA) photo-

chemical bubbling reactor (height 40 cm; I.D. 8 cm) with simulated flue gas generation, absorption and analysis section as depicted in Figure 2.13.

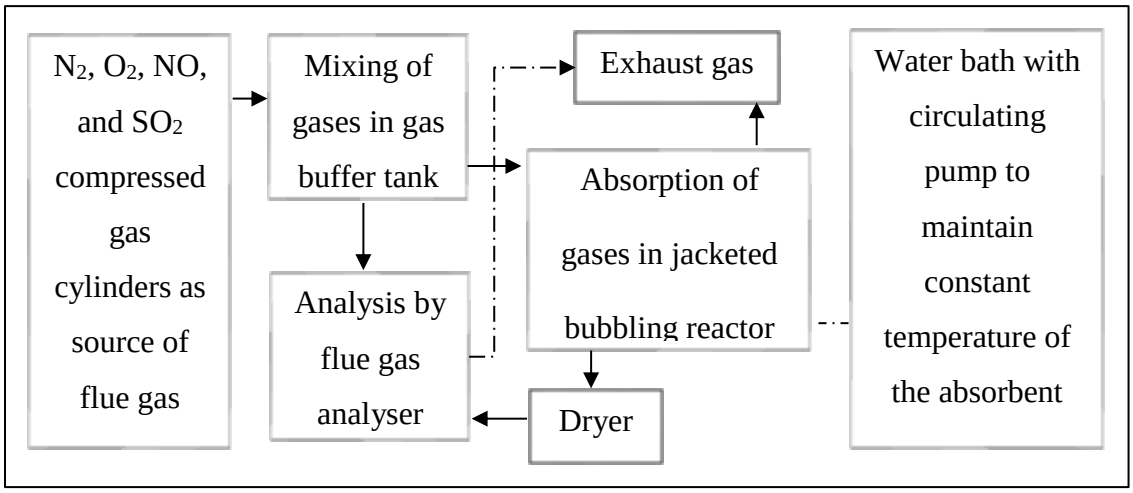

Figure 2.13. Experimental flow sheet for SO_2 and NO removal by advanced oxidation using UV/H_2O_2

The results had shown maximum SO_2 removal of 100 % for all experimental conditions. UV and H_2O_2 had an efficient role in removal of both SO_2 and NO with significant cooperative effect around 6.0. The NO removal efficiency was increased with increase of H_2O_2 concentration and UV lamp power. The material balances of the process for SO_2 and NO were performed and the ion products in the solution were examined by ion chromatography. The reaction pathways for the process were also discussed as follows:

$$SO_2 + H_2O_2 \rightarrow 2H^+ + SO_4^{2-} \quad (2.23)$$

$$HSO_3^- + H_2O_2 \rightarrow SO_4^{2-} + H^+ + H_2O \quad (2.24)$$

$$SO_3^{2-} + H_2O_2 \rightarrow SO_4^{2-} + H_2O \quad (2.25)$$

$$2NO + 3H_2O_2 \rightarrow 2\ H^+ + 2NO_3^- + 2H_2O \quad (2.26)$$

$$NO_2^- + H_2O_2 \rightarrow NO_3^- + H_2O \quad (2.27)$$

2.14. De-SO_2 and De-NO study in bubbling reactor using $NaClO_2$ solution

The simultaneous De-SO_2 and De-NO study in bubbling reactor using $NaClO_2$ solution were carried out by Yi et al., 2009. The experimental apparatus was fabricated by main three parts such as flue gas simulation system, reaction system and flue gas analyser as shown Figure 2.14. A lab scale bubbling reactor (height 15 cm; volume 1 L) had a sampling port at the bottom of the reactor. Primary buffer bottle was used to avoid the conversion of NO to NO_2.

This study was proposed the reaction mechanism by analysing the removal products as follows:

$$NaClO_2 + HCl \rightarrow HClO_2 + NaCl \quad (2.28)$$

$$HClO_2 \rightarrow ClO_2 + Cl_2 + 4H_2O \quad (2.29)$$

$$NaClO_2 + Cl_2 \rightarrow NaCl + ClO_2 \quad (2.30)$$

$$5SO_2 + 2ClO_2 + 6H_2O \rightarrow 5H_2SO_4 + 2HCl \quad (2.31)$$

$$2H_2SO_3 + NaClO_2 \rightarrow 2H_2SO_4 + NaCl \quad (2.32)$$

$$4NO + 3NaClO_2 + 2H_2O \rightarrow 4HNO_3 + 3NaCl \quad (2.33)$$

$$5NO + 3ClO_2 + 2H_2O \rightarrow 5HNO_3 + 3HCl \quad (2.35)$$

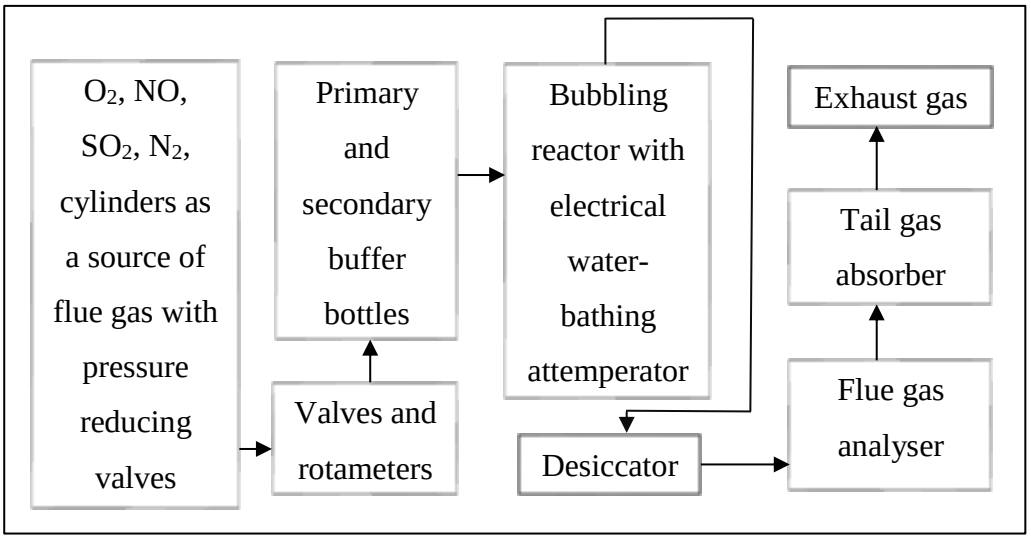

Figure 2.14. Experimental outline of removal of SO_2 and NO by bubbling reactor system using $NaClO_2$ solution

However, the overall reaction of above reaction mechanism of De-SO_2 and De-NO by $NaClO_2$ solution written in equations (2.35) and equation (2.36)**.**

$$2SO_2 + NaClO_2 + 2H_2O \rightarrow 2H_2SO_4 + NaCl \qquad (2.36)$$

Thermodynamics of SO_2-NO-$NaClO_2$ system, reaction kinetics of SO_2 and NO were calculated in this study. The experimental results were observed that at optimum conditions using $NaClO_2$ solution, both SO_2 and NO removal efficiency were 100 and 95%, respectively. SO_4^{2-} and NO_3^- were predominant product during De-SO_2 and De-NO, respectively.

2.15. Removal in an integrated wet scrubber-electrochemical cell system

Pilli et al., 2009 investigated the experimental aspects of combined removal of NOx and SO_2 from flue-gas in an integrated wet scrubber-electrochemical cell system. The major

concern of this work was to investigate the parametric tests of some operating conditions on the combined removal of NO_x and SO_2 from simulated flue gas stream in a scrubber column (length 1.2 m; I.D. 0.05 m; height 0.8 m) with packing material as described in Figure 2.15**.**

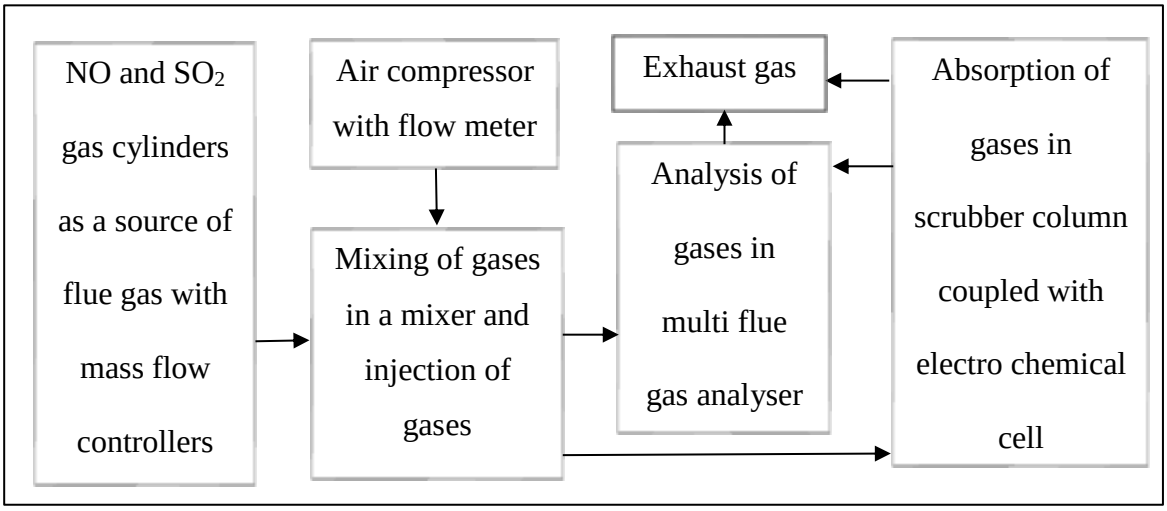

Figure 2.15. Process flow sheet of SO_2 and NO removal in an integrated wet scrubber-electrochemical cell system.

The electrochemical cell used in this study was plate-and frame type with narrow gap divided into flow cell configuration. During the process, the gaseous components were absorbed into 6 M HNO_3 electrolyte in the scrubber in a counter-current mode, and were removed by the Ag (II) mediator oxidant electrochemically generated in an electrochemical cell set-up. The influencing parameters such as packing material, feed concentrations of NO and SO_2, superficial gas velocity and liquid velocity were studied for combined removal of SO_2 and NO. NO removal was maximum with high surface area

raschig glass rings. Increase in feed concentration reduced the NO and NO_x abatement. Nitrogen components removal was faster with SO_2 co-existed in the feed. Increase in gas flow rate decreases the removal efficiency of both gasses and completely reverse for liquid flow rate.

2.16. Removal of NO from simulated gas in a bubbling reactor using aqueous ClO_2

This work was attempted by Deshwal et al., 2008 to clean up NO from flue gas in aqueous chlorine-dioxide solution (ClO_2) using lab-scale bubbling reactor. Chloride-chlorate process was used to generate the ClO_2 from acid solutions of either sodium chlorate or sodium chlorite as follows:

$$ClO_3^- + 2H^+ + e^- \rightarrow ClO_2 + H_2O \quad (2.37)$$

$$2H^+ + 2ClO_3^- + 2Cl^- \rightarrow 2ClO_2 + 2Cl_2 + 2H_2O \quad (2.38)$$

$$2ClO_2 + H_2O_2 + 2NaOH \rightarrow 2NaClO_2 + O_2 + 2H_2O \quad (2.39)$$

$$2ClO_2 + 2NaOH \rightarrow 2NaClO_2 + NaClO_3 + H_2O \quad (2.40)$$

NO was finally converted into nitrate (NO_3^-) and ClO_2 was reduced into chloride (Cl^-) ions. The reactions for NO_x removal, SO_2 removal may be written as:

$$5NO + 3ClO_2 + 4H_2O \rightarrow 5NHO_3 + 3HCl \quad (2.41)$$

$$NO + Cl_2 + H_2O \rightarrow NO_2 + 2HCl \quad (2.42)$$

$$NO + 3Cl_2 + 4H_2O \rightarrow 2NHO_3 + 6HCl \quad (2.43)$$

$$5SO_2 + 2ClO_2 + 6H_2O \rightarrow 5H_2SO_4 + 2HCl \quad (2.44)$$

$$5NO + 3ClO_2 + 4H_2O \rightarrow 5NHO_3 + 3HCl \quad (2.45)$$

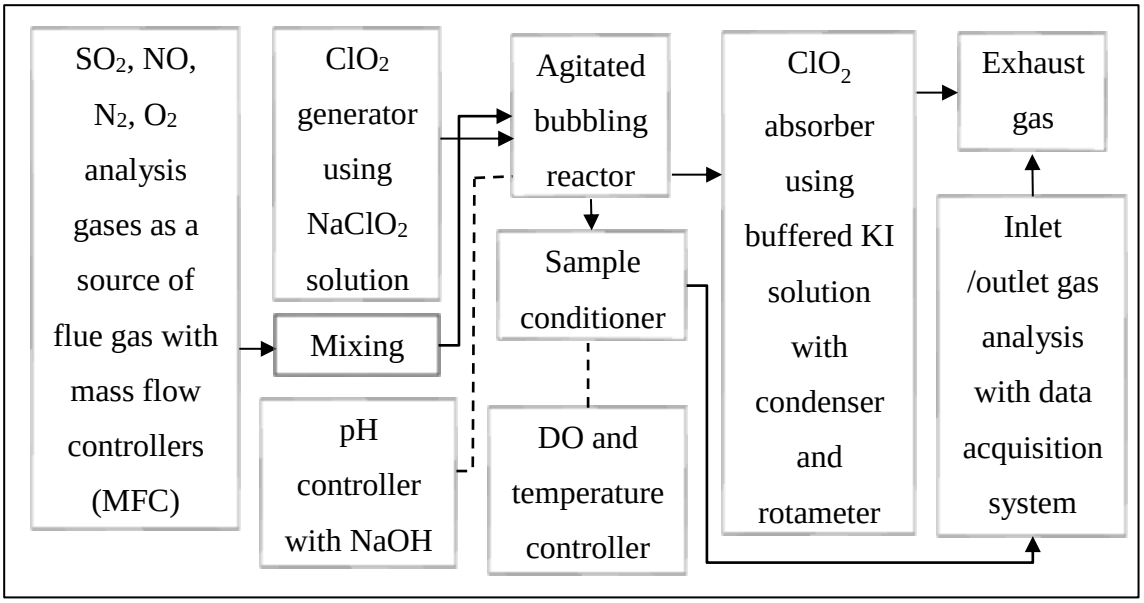

Figure 2.16. Schematic diagram for NO removal in bubbling reactor using aqueous ClO_2 scrubbing

The experimental set-up was composed of two units mainly chlorine-dioxide generation system and flue gas cleansing system as outlined in Figure 2.16. The flue gas cleansing system included analysis gases, agitated bubbling reactor, DO, pH and temperature control system, ClO_2 absorber, sample cum analysis and data acquisition system. The bubbling reactor (I.D 15 cm; height 45 cm) was made of acrylic material.

All experiments were resulted to find out the effect of various operating parameters like input NO concentration, NaCl feeding rate, time, pH of the solution, presence of SO_2 and inital SO_2 concentration on the NOx removal efficiency. The NO_x removal efficiency improved slightly with the increasing input NO concentration as well as presence of SO_2.

The optimum NO_x removal efficiency of approximately 60% had been achieved under pH range of 3–11.

2.17. Absorption using Fe^{II} EDTA combined with Na_2SO_3 solution

Wang et al., 2007 investigated the reaction mechanism and reaction products during simultaneous absorption of NO and SO_2 in Fe^{II} EDTA combined with Na_2SO_3 solution using cyclic voltammetry and Raman spectroscopy. The process was done in a double-stirred vessel attached (I.D. 76 mm, height 150 mm) with water jacket for controlling the inner temperature of the reactor according to the Figure 2.17.

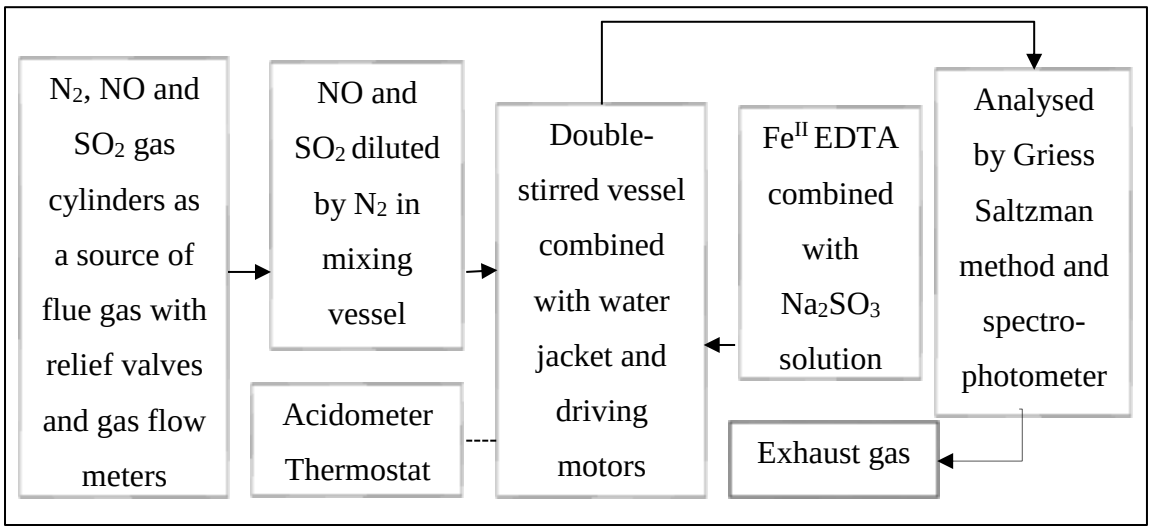

Figure 2.17. Absorption of SO_2 and NO in double-stirred vessel using Fe^{II}(EDTA) combined with Na_2SO_3 solution

Four stainless steel baffles (height 129 mm, width 5 mm) were used to stirrer the both liquid and gas phase. It was observed that the presence of SO_2 enhanced the period of

high efficiency (greater than 60%) of NO absorption by 1.59 times and raised 36.65% absorption capability of NO within 500 min. This is due to NO reduction by SO_2 before getting into Fe^{II} EDTA combined with Na_2SO_3 solution. The accession of Na_2SO_3 provided the SO_3^{2-} which regenerated of Fe^{II} EDTA solution and maintained the pH value of the solution. The reductions of Fe^{II} EDTA(NO), Fe^{III} EDTA and NO absorption were major reactions in the process system as follows:

$$2NO + 2Fe^{II}EDTA + 2H^+ \rightarrow N_2O + 2Fe^{III}EDTA + H_2O \quad (2.46)$$

$$Fe^{2+} + OH^- \rightarrow Fe(OH)_2 \quad (2.47)$$

$$NO + NO_2 + H_2O \rightarrow 2HNO_2 \quad (2.48)$$

$$2Fe^{II}EDTA(NO) + SO_3^{2-} \rightarrow 2Fe^{II}EDTA + (NO)_2SO_3^{2-} \quad (2.49)$$

$$(NO)_2SO_3^{2-} \rightarrow N_2O + SO_4^{2-} \quad (2.50)$$

$$2NO + SO_2 \rightarrow N_2O + SO_3 \quad (2.51)$$

$$Fe^{III}EDTA + e^- \rightarrow Fe^{II}EDTA \quad (2.52)$$

$$NO_3^- + 4H^+ + 3e^- \rightarrow NO + 2H_2O \quad (2.53)$$

$$2Fe^{II}EDTA(NO) + 2H^+ + 2e^- \rightarrow H_2O + N_2O + 2Fe^{II}EDTA \quad (2.54)$$

2.18. Removal of SO_2, NO and particulate using Fe(II)-EDTA in pilot-scale scrubber

The simultaneous removal efficiency of SO_2, NO and particulate in pilot-scale scrubber system was evaluated by ferrous chelate (Fe(II)-EDTA) as wet absorbent (Fe(II)-EDTA 0.03 M, ascorbic acid 0.024 M, adipic acid 0.024 M, sodium sulphite 0.09 M) (Jung et al., 2007**)**. In this work, the experimental system included either a small-scale incinerator

or flue gas simulation system, scrubber with control box, tower sump, particulate generator and lastly dust mate and toxic gas analyser **(**Figure 2.18**)**. The laboratory scale scrubber (I.D. 0.18 m, O.D. 0.20 m, height 2.25 m) was made of acrylic material. It had a nozzle for the spraying the wet absorbent and pall ring used as packing material in two stage structure (size 5/8 or 1.0 in.) for stacking.

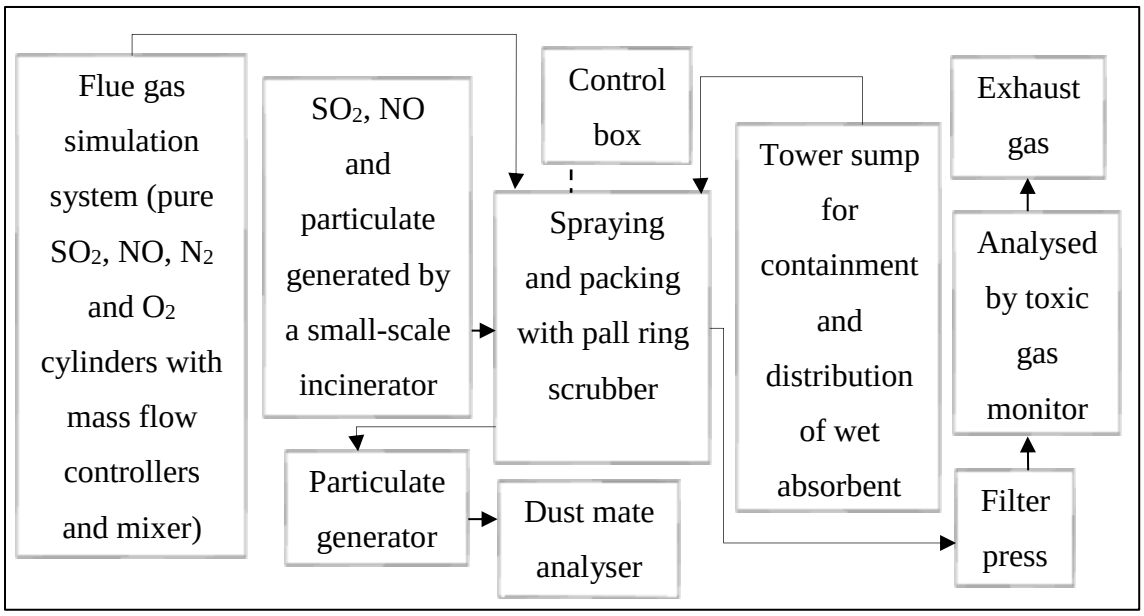

Figure 2.18. Flow diagram for removal of SO_2, NO and particulate by scrubber system using wet absorbent

This work was evaluated the effects of stage number of scrubber, liquid-gas ratio and type of packing material with regard the removal of SO_2, NO and particulate; and effect of nozzle and wet absorbent flow rate on particulate removal. The maximum particulate and SO_2 were found out at least 96-98%. In one-stage scrubber, after 48 hours removal efficiency of NO was reached; however, an NO removal efficiency of 95.7% was attained

in the two-stage scrubber. The particulate and SO_2 removal efficiency were achieved higher than 98% using STS and P.P. pall ring as packing material in the scrubber column; however, NO removal was differed with the different packing materials tested.

2.19. Removal by using ozone injection and absorption–reduction technique

Mok and Lee, 2006 investigated simultaneous absorption by a two-step process which can remove NO_x and SO_2. This process consists of an ozonizing chamber (I.D. 5 cm; Length 25 cm) and a wet scrubber agitated vessel containing an absorbing agent solution. Here air is used as source of ozone in ozonizing chamber.

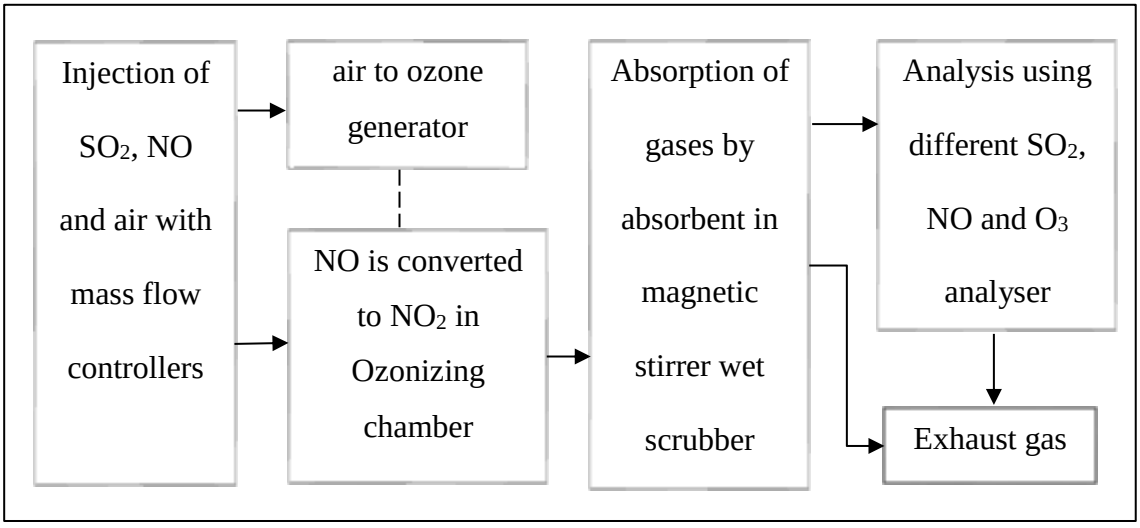

Figure 2.19. Process flow sheet for SO_2 and NO removal by using ozone injection and absorption–oxidative technique.

The experimental setup consists of four major units such as preparation of simulated gas stream, ozone generation, absorption chamber and analysis units as illustrated in Figure

2.19. The injection of ozone into the simulated gas promotes the rapid oxidation of NO to NO_2. Sodium sulfide (Na_2S) is used as the absorbing agent in this study which can effectively remove SO_2. A dielectric barrier discharge device using AC high voltage was employed as the ozone generator, and Na_2S was used as the absorbing agent. Throughout the process the effective NO_x removal efficiency was obtained as about 95 and 100 % removal efficiency of SO_2 was observed. Ozonizing chamber is for the oxidation of NO where NO in the simulated gas was oxidized to NO_2 by the following reactions:

$$NO + O_3 \rightarrow NO_2 + O_2 \quad (2.55)$$

$$2NO_2 + Na_2S \rightarrow Na_2SO_4 \quad (2.56)$$

When the simulated gas treated by ozone and forwarded to the absorber, SO_2 can be removed by Na_2S as follows:

$$2SO_2 + N_2S \rightarrow 2S + Na_2SO_4 \quad (2.57)$$

2.20. Absorption in hexamine cobalt(II)/iodide solution

The feasibility of an innovative process catalyst system merged with absorption chamber for simultaneous removal of SO_2 and NO from combustion flue gas was investigated Long et al., 2005. This catalyst system was introduced to the scrubbing ammonia solution to provide sequential catalytic oxidation and absorption for combined removal of SO_2 and NO in the same reactor. In the process of catalytic reduction, $Co(NH_3)_6^{2+}$ ions provide the catalytic activity where as I^- ions act as the co-catalyst. During the oxidation process, residual oxygen in the gas reaches equilibrium with dissolved oxygen in liquid. The experiments were carried out in a bubble column (I.D. 18 mm; length 1000 mm) and packed column (I.D. 18 mm; length 1000 mm) as shown in Figure 2.20.

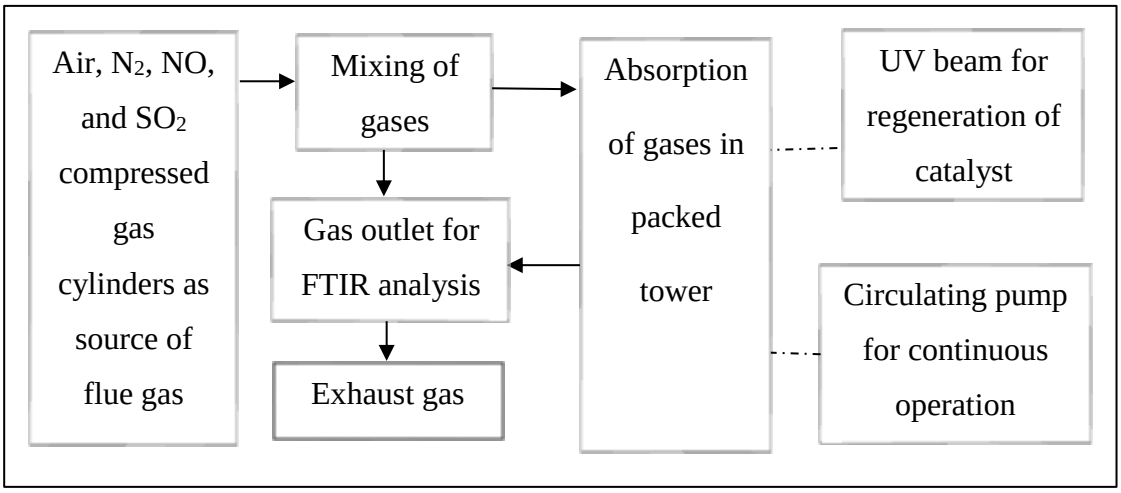

Figure 2.20: Experimental flow sheet for absorption of SO_2 and NO in hexamine cobalt(II)/iodide solution

The effects of major operating parameters such as oxygen flow, different amounts of absorbents, ultraviolet irradiation and SO_2 concentration were investigated during the combined absorption of SO_2 and NO. The removal efficiency was enhanced by UV irradiation at 365 nm. At feed concentration of 250–900 ppm the NO removal is greater than 95%. But for SO_2 removal at a feed concentration of 800–2500 ppm was nearly 100%. The SO_2 concentration change raises the NO removal efficiency. The end products obtained during the process were ammonium sulphate and ammonium nitrate as these compounds were important ingredients to be used as fertilizer materials and their reaction mechanisms were given as follows:

$$NO + SO_2 + 3/2\ H_2O + 3NH_3 + O_2 \rightarrow ½\ NH_4NO_2 + ½\ NH_4NO_3 + (NH_4)_2SO_4 \qquad (2.58)$$

2.21. Modelling of mass transfer during absorption with chemical reaction

Susianto et al., 2005 studied a model for mass transfer in simultaneous absorption of SO_2 and NO_2 involving chemical reactions. During the experimentation, the simultaneous absorption of SO_2 and NO_2 was carried out in a gas–liquid stirred tank reactor at low temperature of 298 K. Here the gas flow was operated in continuous mode whereas batch operation for the liquid phase. The schematic flow sheet of the process was shown in Figure 2.21.

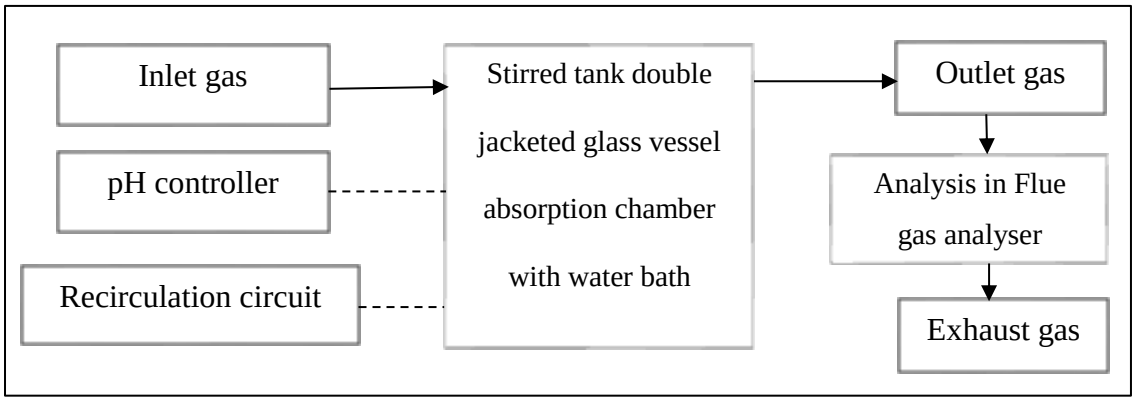

Figure 2.21. Process flow sheet for absorption of SO_2 and NO_2 in water

The absorption kinetics of SO_2 and NO_2 was mainly influenced by the solution pH. Absorption of SO_2 was faster than absorption of NO_2 in weak acid. The combined absorption between the generated ions concludes the formation of N_2O and hydroxylamine di-sulfonic acid. Nitrite and sulphite ions enhance the mass transfer for NO_2. The considered reactions for modelling were as follows:

$$NO_2^- + 2HSO_3^- + H^+ \Leftrightarrow HON(SO_3)_2^{2-} + H_2O \qquad (2.59)$$

$$2NO_2 + H_2O \rightarrow NO_2^- + NO_3^- + 2H^+ \quad (2.60)$$

$$SO_2 + H_2O \rightarrow HSO_3^- + H^+ \quad (2.61)$$

2.22. Absorption of SO_2 and NO_x in acidic $NaClO_2$ solution under spraying column

The kinetics study on absorption SO_2 and NO from simulated flue gas as per desired coal-fired power plant system by sodium chlorite ($NaClO_2$) solution using a lab-scale spraying column was done by Chen et al., 2003. All absorption experiments were done in a lab-scale spraying scrubber column (I.D. 5 cm, length of reaction zone 10 cm), which had three-piece uni-jet type spray nozzle. The schematic diagram of process system is shown in Figure 2.22, which consists of the flue gas simulation system, two stage mixers (O.D 5 cm; length 12 cm), heater, spray scrubber, pump and rotameter.

This study was involved the effect of NO_x concentration, gas-liquid contact time, $NaClO_2$ concentration, initial pH and operating temperature on NO_x absorption rate; effect of NO_x concentration, SO_2 concentration and $NaClO_2$ concentration on simultaneous SO_2 and NO_x absorption rate; activation energy; and reaction order of NO and $NaClO_2$ concentration. The reactions involved in this study were summarized as below:

$$NaClO_2 \rightarrow Na^+ + ClO_2^- \quad (2.62)$$

$$2NO + ClO_2^- \rightarrow 2NO_2 + Cl^- \quad (2.63)$$

$$NO + ClO_2^- \rightarrow NO_2 + ClO^- \quad (2.64)$$

$$4NO_2 + ClO_2^- + 4OH^- \rightarrow 4NO_3^- + Cl^- + 2H_2O \quad (2.65)$$

$$2NO_2 + ClO_2^- + 2OH^- \rightarrow 2NO_3^- + ClO^- + H_2O \quad (2.66)$$

$$4ClO_2^- + 2H^+ \rightarrow 2ClO_2 + ClO_3^- + Cl^- + H_2O \quad (2.67)$$

This study resulted that the range of absorption rate was occurred between 1.91×10^{-11} and 9.59×10^{-10} mol s^{-1} cm^{-2}, the range of rate constant was measured between 1.32×10^{7} and 1.21×10^{8} (L mol^{-1})$^{1.9}$ s^{-1}, and average rate constant, activation energy and frequency factor were 6.16×10^{7} (L mol^{-1})$^{1.9}$ s^{-1}, 129 kcal/mol and 6.93×10^{16} (L/mol)$^{1.9}s^{-1}$, respectively.

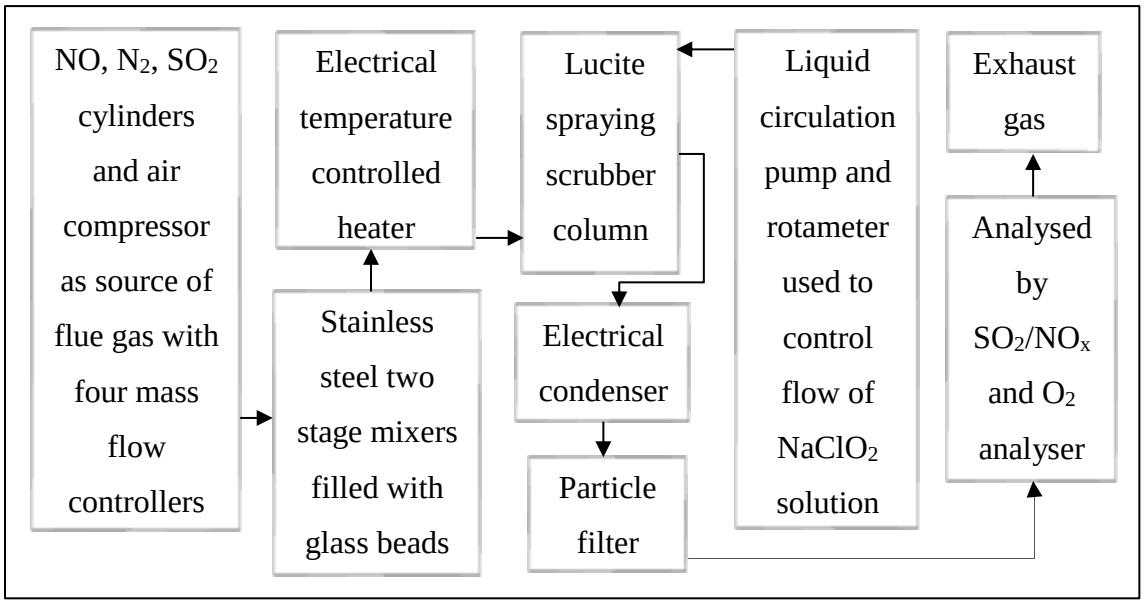

Figure 2.22. Absorption of SO_2 and NO_x in spraying scrubber using acidic $NaClO_2$ solutions

2.23. Absorption using $KMnO_4$/NaOH solutions

According to the research work conducted by Chu et al., 2001 the feasibility of $KMnO_4$/NaOH absorbent for simultaneous removal of SO_2 and NO was examined in an advanced air pollution controlling device of wet scrubbing. This process also explained

the absorption kinetics to scale up the process. The process is carried out in a stirred tank reactor (I.D. 8 cm; height 18 cm) containing impeller for agitation of the solution as shown in the Figure 2.23**.**

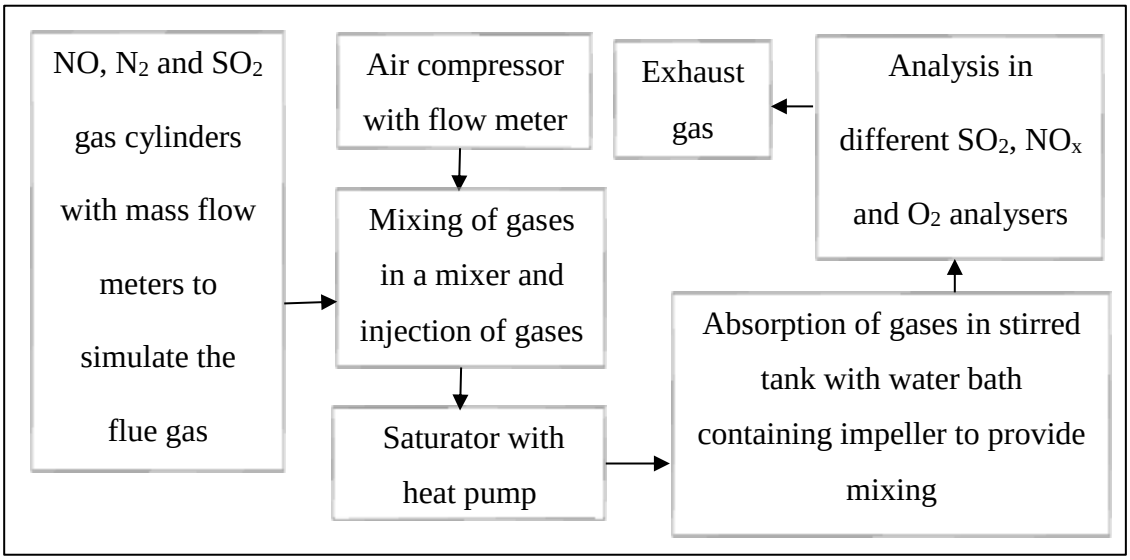

Figure 2.23. Process flow sheet for absorption of SO_2 and NO using $KMnO_4$/NaOH solutions

The experiment was performed at 323 K and the film mass transfer coefficients for gas and liquid were determined for the process. When the concentration of NaOH and $KMnO_4$ were greater than 0.1 M and 0.05 M, respectively, then absorption of SO_2 tends to gas film controlling. Positive effect has been observed for SO_2 removal with raise in gas flow rate. Presence of O_2 also acts as promoter for SO_2 removal. But addition of SO_2 reduces absorption rate of NO. The major reactions occurred during the absorption of SO_2 and NO with $KMnO_4$/NaOH were given below:

$$MnO_4^- + NO + 2OH^- \rightarrow MnO_4^{2-} + NO_2^- + H_2O \quad (2.68)$$

$$2MnO_4^- + NO_2^- + 2OH^- \rightarrow 2MnO_4^{2-} + NO_3^- + H_2O \quad (2.69)$$

$$2MnO_4^- + 3NO_2^- + 2OH^- \rightarrow 2MnO_2 + 3NO_3^- + H_2O \quad (2.70)$$

$$MnO_4^- + NO + 2OH^- \rightarrow MnO_2 + NO_3^- \quad (2.71)$$

$$2MnO_4^- + SO_3^{2-} + H_2O \rightarrow 2MnO_4^- + SO_4^{2-} + 2OH^- \quad (2.72)$$

Table 2.1. summarizes the maximum removal efficiencies for SO_2 and NO from the gas stream available in literature. It also includes the operating conditions, absorbents and columns used by various researchers.

2.24. Research Gap

The summary of research work in the literature is given in Table 2.1. The various wet scrubbers were used for simultaneous removal of SO_2 and NO from waste gas streams. Among these, the most important scrubbers are spray column, packed column, plate column, impingement type scrubber, multi-stage bubble column, multi-jet column and the venturi-scrubber. All these wet processes have done tremendous job in terms of removal efficiency using various absorbents, but the disposal of spent absorbent is still a problem. The conversion of these toxic gases SO_2 and NO into useful products is the running issue. The present research is focussed on efficient removal of both SO_2 and NO during simultaneous absorption and to use the suitable absorbent for getting the valuable products. The exhausted absorbent may be used as fertilizers for agricultural purposes, which discards the disposal problem of the spent absorbent.